

Start-to-end Simulation for the LCLS Xray-FEL*

S. Reiche, C. Pellegrini, J. Rosenzweig, UCLA, Los Angeles CA 90095, USA
P. Emma, P. Krejcik, SLAC, Stanford, CA 94309, USA

Abstract

X-ray FELs, such as the LCLS and TESLA FEL, require electron beams with large peak current and very small emittance. The X-ray peak power, temporal and spectral properties, depend significantly on details of the electron beam phase space distribution. The electron beam distribution is determined by many effects, as the emission process at the gun photo-cathode, bunch compression, acceleration and wakefields within the undulator. Although analytical results can give an estimate of the expected performance, the complexity of the electron beam generation, acceleration and compression can only be evaluated using a numerical simulation of all these processes, a start-to-end simulation. In this presentation we discuss the LCLS X-Ray FEL performance estimated by a start-to-end simulation, and we compare the results with those obtained using a simpler model.

1 INTRODUCTION

Many Free-Electron Laser experiments have confirmed the SASE FEL principle down to a wavelength of 80 nm [1]-[10]. For those experiments and the future X-ray FEL projects at LCLS[11] and TESLA[12] a good electron beam quality is essential for optimal performance. The resulting requirements for beam emittance and energy spreads at high peak current become more stringent for shorter wavelength which typically scale with the FEL parameter ρ [13].

A high-brightness rf photo-electron gun produces beam emittances below 2 mm-mrad and an energy spread around 10 keV. These quantities have to be conserved while accelerating, compressing and transporting the beam to the undulator. Various aspects degrades the beam quality such as space charge forces and efficiency of the emittance compensation scheme in the injector section as well as wakefields and CSR effects in the linac and compressor. During the FEL amplification wakefields generated by the undulator vacuum chamber can shift parts of the electron beam out of the FEL bandwidth. In addition a slippage length much shorter than the bunch length couples strongly the FEL output profile with the variation of mean energy, emittance, current, energy spread and mismatching along the bunch.

In this presentation we show the results for the first consistent start-to-end simulations for the LCLS X-ray FEL. The simulations are done for two cases. The first case models the LCLS design parameters (see Tbl. 1). Emittance scaling[14] shows that an operation at lower charge

is more favorable. Thus the second case is optimized at a bunch charge of 0.25 nC.

Particle tracking through the LCLS beam line is done in three stages. The first stage applies the computer code PARMELA[15] for tracking from cathode to 150 MeV at the injection point into the SLAC linac. After this point, the high-energy beam is insensitive to space charge forces and the tracking code ELEGANT[16] is used up to 14.3 GeV at undulator entrance. ELEGANT includes wakefields, bunch compression, CSR, 2nd-order aberrations, component misalignments, and trajectory correction. The tracking is done using 200k macro-particles and is repeated for various charge levels after system re-optimization. The final stage is FEL simulation using Genesis 1.3[17]. The large number of macro-particles allows the bunch to be 'sliced' 50-100 times so that the emittance, peak current, and energy spread can be evaluated all along the 230-fsec bunch length while resolving the electron distribution on the Ångström level with GENESIS 1.3 internal distribution of macro-particles.

Table 1: LCLS Parameters

Electron Beam	
Beam energy	14.4 GeV
Relative energy spread	$6 \cdot 10^{-5}$
Normalized emittance	1.2 mm·mrad
Charge	1 nC
Peak current	3.4 kA
Undulator	
Undulator period	3 cm
Undulator field	1.3 T
Undulator parameter K	3.7
Undulator length	122 m
Focusing beta function	18.0 m
FEL	
Resonant wavelength	1.5 Å
FEL parameter ρ	$5 \cdot 10^{-4}$
Saturation length	86 m
Saturation power	18 GW

2 THE INJECTOR

The LCLS injector — a 1.6 cell S-band rf-photo gun and a succeeding acceleration section — boost the electron energy up to 150 MeV. The operation point for emittance compensation yields a slice emittance of 0.5 and 0.3 mm-mrad for the two cases, respectively. The simulation includes contributions by the thermal emittance, which tends to smooth out the transverse phase space distribu-

* work supported by DOE contract DE-AC03-76SF00515

tion and thus reduce the effects of beta-mismatch along the bunch. The second case is optimized for minimum emittance by reducing the charge, where the space-charge emittance and thermal emittance are of the same amplitude. The resulting charge is 0.25 nC. Effects of chromatic and rf-focusing are negligible.

The simulations does not take into account effects such as non-uniform illumination of the photo-cathode or non-uniform photo-electron emission.

3 THE LCLS BEAM LINE

The acceleration and compression systems have been designed in order to: 1) generate the high peak current and beam energy required for SASE; 2) mitigate beam-brightness degrading effects such as wakefields in the linac and coherent synchrotron radiation (CSR) in the bends; and 3) minimize the sensitivity of final bunch length and energy to charge and gun-laser timing jitter. Special systems have been incorporated, such as a double-chicane compressor to reduce CSR-induced emittance growth, and a 4th-harmonic compression linearizer using X-band RF. The design is flexible enough to allow operational re-optimization for different bunch charge settings.

Fig. 1 shows the sliced beam properties at 14.4 GeV for the 1 nC and 0.25 nC case (top and bottom plots, respectively) for various cuts in the transverse phase space. The parameter $\langle R_4 \rangle$ is an indicator for time-dependent centroid offsets in the transverse dimension and is in units of rms beam size. The consequences of a beam mismatch along the bunch as well as variation in the emittance, energy spread and current are discussed in the next section. The variation of the mean energy along the bunch yields a wider bandwidth of the observed radiation spectrum than that given by the SASE FEL process itself.

4 THE LCLS UNDULATOR

Although the LCLS undulator has thousands of periods, the total slippage length is within approximately 500 nm, much smaller than the bunch length of 80 μm . Thus different sections (slices) of the bunch interact with the radiation independently. Any projected value of beam parameters such as emittance or energy spread loses its merit to describe the FEL amplification.

Prior to running GENESIS 1.3 the longitudinal distribution is used to calculate the wakefields within the undulator vacuum pipe. We take resistive wall[18] and surface roughness[19] wakefields into account for a copper plated vacuum pipe of 5 mm diameter. The roughness has an rms amplitude of 100 nm and a radial to longitudinal aspect ratio of 1:500. The wakefields are dominated by the resistive wall component.

Fig. 2 shows the wakefield potential for the 1 nC case (solid line). The amplitude is roughly twice as large as that (dashed line) for a stepped profile using the LCLS design parameters. The enhancement is caused by the spike at the

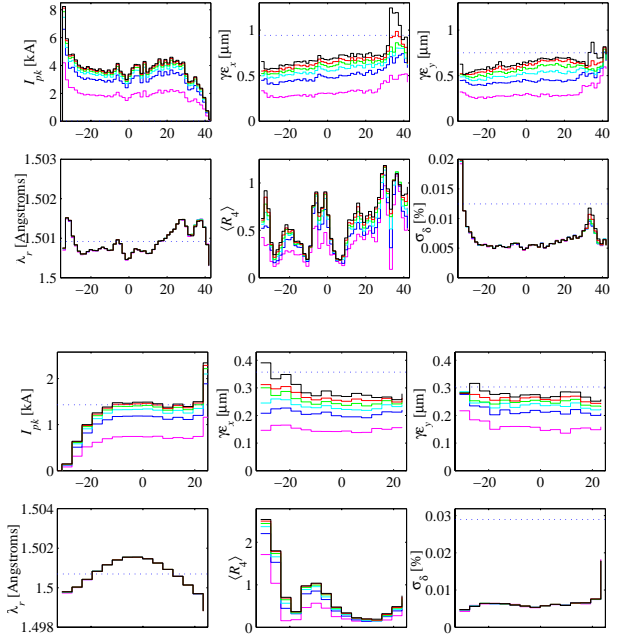


Figure 1: Beam properties for 1 and 0.25 nC (top 6 and bottom 6 plots, respectively) in units of microns along the bunch. In each plot the curves from the top to the bottom corresponds to 0%, 2%, 5%, 10%, 20% and 50% cuts in the transverse phase space.

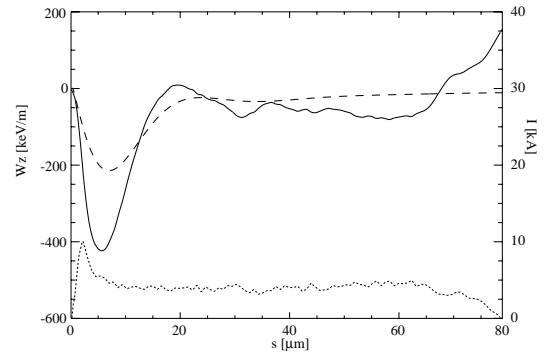


Figure 2: Wake potential for the start-to-end and step profile (solid and dashed line, respectively) and current profile (dotted line).

head of the current distribution (dotted line), which arises due to non-linear term in the bunch compression. Because the width of this spike is shorter than the characteristic length of all wakefield components the spikes contributes coherently to the total wakefields. Concerning a minimal degradation by wakefields, the X-band compensation during bunch compression eliminates those spikes in the head region of the bunch, but not to all orders.

The GENESIS 1.3 simulation saturates after 65 m at an average saturation power level of 16 GW and 25 GW depending on whether wakefields are included or not. Thus

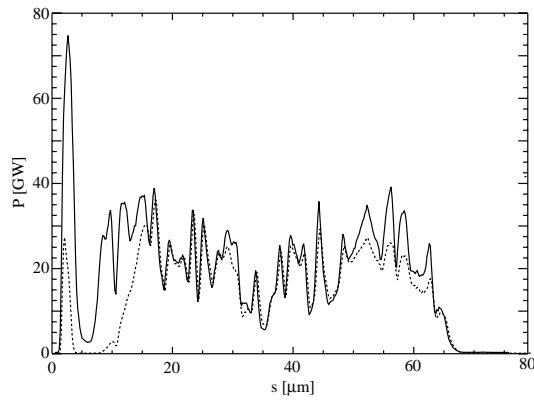


Figure 3: Longitudinal radiation profile at saturation with and without wakefields (dotted and solid line, respectively).

the performance exceeds that of the LCLS design parameters with a saturation length of 85 m and a saturation power of 10 GW (18 GW without wakefields). Because the gain length depends strongly on the emittance, the smaller slice emittance of about 0.5 mm-mrad in the core of the beam improves the LCLS performance. This enhancing effect is only partly compensated by wakefields and time-dependent beam mismatch. Fig. 3 shows the longitudinal radiation profiles at saturation for simulations with and without wakefields. The major impact of wakefields are noticeable in the head part of the bunch (left). This is in coincidence with a large wakefield amplitude of 400 keV/m (Fig. 2). The tail of the bunch does not saturate because the slice emittance is about twice as large as those in the core of the beam. In addition the current drops below 3 kA.

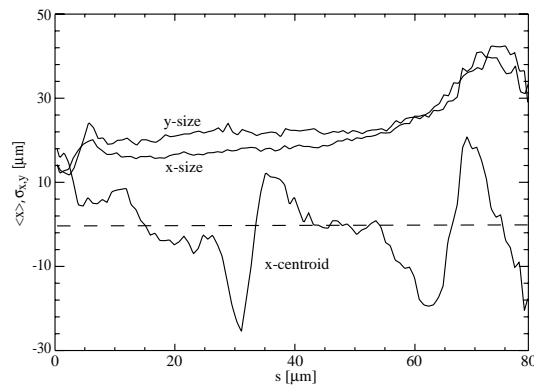


Figure 4: Beam sizes and centroid position for the 1 nC case.

Although the current and the emittance are almost constant along the center part of the bunch, the radiation profile has a noticeable reduction around $s = 35 \mu\text{m}$. It has its origin in the transverse centroid motion of this part of the bunch, $\langle R_4 \rangle$. The matching to the undulator focusing lattice can only be done for the projected phase space ellipse of the electron beam. The betatron oscillation of individual slices can get as large as the rms size of the

beam size (see Fig. 4). Wakefield and CSR effects in the LCLS beam line are causing this displacement of the centroid along the bunch.

The simulation of the lower charge case benefits from various aspects. First the slice emittance is lower, which allows us to increase the focusing strength and thus the electron density. Second the wakefields are reduced due to the lower current and the lack of any spikes at the head of the bunch. The FEL saturates at 53 m at a power level of 12 GW.

5 CONCLUSION

The output of the LCLS X-ray FEL for the start-to-end simulations differs significantly from those based on the LCLS design parameters. It emphasize the importance of such kind of simulation.

Local parts of the electron bunch amplify the spontaneous radiation differently resulting in a strong fluctuation of the FEL output power on the longitudinal scale of wakefields, CSR and space-charge effects. This makes any analyses of the measured FEL performance more difficult if the diagnostics average over the entire pulse. In particular the radiation bandwidth due to the correlated energy spread is larger than the FEL bandwidth.

The simulations also show that an operation point at 0.25 nC instead of 1 nC is favorable. Most degrading effects such as CSR are reduced while the tolerances for the LCLS beam line become more relaxed.

6 REFERENCES

- [1] T. Orzechowski *et al.*, Phys. Rev. Lett. **55** (1985) 889
- [2] R. Prazeres *et al.*, Phys. Rev. Lett. **78** (1997) 2124
- [3] M. Hogan *et al.*, Phys. Rev. Lett. **80** (1998) 289
- [4] M. Babzien *et al.*, Phys. Rev. **E57** (1998) 6093
- [5] D.C. Nguyen *et al.*, Phys. Rev. Lett. **81** (1998) 810
- [6] M. Hogan *et al.*, Phys. Rev. Lett. **81** (1998) 4867
- [7] L.-H. Yu *et al.*, Nucl. Inst. & Meth. **A445** (1999) 301
- [8] S.V. Milton *et al.*, Phys. Rev. Lett. **85** (2000) 988
- [9] J. Rossbach *et al.*, Phys. Rev. Lett. **85** (2000) 3825
- [10] A. Tremaine *et al.*, Presented at this Conference
- [11] LCLS Design Study Report, Report SLAC-R-521 (1998)
- [12] J. Rossbach *et al.*, Nucl. Inst. & Meth. **A375** (1996) 269
- [13] R. Bonifacio, C. Pellegrini and L. Narducci, Opt. comm. **50** (1984) 373
- [14] J.B. Rosenzweig and E. Colby, Proc. of the ACC Conference, **AIP 335** (1995) 724
- [15] L.M. Young and J.H. Billen, *PARMELA*, LA-UR-96-1835 (2000)
- [16] M. Borland, Proc. of the ICAP-2000 Conference, Darmstad (2000)
- [17] S. Reiche, Nucl. Inst. & Meth. **A429** (1999) 243
- [18] K. Bane, SLAC report AP-87 (1991)
- [19] K. Bane and G.V. Stupakov, SLAC report, SLAC-PUB-8599 (2000)